AppliedPhotophysics
Ultrasensitive Spectroscopy for the Life Sciences

SX SERIES APPLICATION NOTE

Stopped-Flow Fluorescence (Förster) Resonance Energy Transfer (FRET)

Abstract: Stopped-flow FRET is a useful technique for studying many types of biomolecular interactions. The method provides kinetic information regarding distance changes occurring on the millisecond timescale. This article gives an introduction to the technique along with a review of some example experiments from the scientific literature. Applied Photophysics can provide the accessories and application support required to perform such experiments on the SX series of stopped-flow spectrometers.

INTRODUCTION

FRET is a phenomenon that can be observed between two fluorophores in which the emission wavelength of a "Donor" species (**D**) overlaps with the absorption wavelength of "Acceptor" species (**A**). Depending on several factors, a transfer of energy may occur from the excited state of **D** (**D***) to the ground state of **A**. This may be observed experimentally as an increase in fluorescence intensity at **A**'s emission wavelength and/or a decrease in intensity at **D**'s emission wavelength. Applied Photophysics offers dual fluorescence stopped-flow capabilities, enabling the measurement of both **D*** and **A*** emissions.

FRET is a useful tool as it is distance dependant; its measurement can give information regarding the dynamics of molecular interactions. Stopped-flow FRET experiments can provide unique information of many types of biomolecular interactions on a millisecond to second timescale.

Authors
James Law, PhD

KEYWORDS

- Stopped-flow
- FRET
- Dual Fluorescence
- Time dependent Spectroscopy
- SX20
- Rapid mixing
- Biomolecular interactions
- Reaction kinetics

BACKGROUND

The energy transfer in FRET is non-radiative and stems from dipole-dipole interactions between **D*** and **A**. FRET can therefore only occur if the orientations of electronic dipoles are largely parallel to each other. This is not usually a problem in solution as the molecules are likely to be at least partially free to rotate allowing the alignment of dipoles. Additionally, the lifetime of **D*** needs to be on a long enough timescale to allow the transfer of energy. Crucially, FRET will only occur at short distances, typically <10 nm and the extent of energy transfer is highly sensitive to the distance between the interacting dipoles. The relationship between the efficiency of the energy transfer (E_{FRET}) and the distance between the donor/acceptor pair (r) follows an inverse 6th power law. E_{FRET} is described by equation (1). E_{FRET} corresponds to the ratio of FRET events per excitation of **D**.

$$E_{FRET} = \frac{R^6_0}{(R^6_0 + r^6)} \quad (1)$$

R_0 is a constant for the donor/acceptor pair known as the Förster radius and is defined as the distance at which E_{FRET} = 50%. It is therefore possible to attribute changes in observed fluorescence intensity to changes in distances between donor/acceptor pairs. The general mechanism of stopped-flow FRET experiments is to label two different biomolecules with separate fluorophores of a donor/acceptor pair. Rapidly mixing a solution of these labelled biomolecules with particular species may then give rise to a change in the FRET signal. Variants on this may be implemented; for example, labelling one biomolecule with both components of the donor/acceptor pair allows the intramolecular dynamics of the macromolecule to be investigated.[1]

IMPLEMENTATION

An initial consideration in performing a stopped-flow FRET experiment is determining where to place fluorophores in the macromolecular system that is to be studied. Ideally, this needs to be at positions which will, based on a given hypothesis, exhibit large changes in distance between donor and acceptor. Fortunately, when studying nucleic acids, it is generally possible to insert a fluorophore at any point in the nucleotide chain. However, it is more difficult to introduce a label into a protein as only surface cysteine residues can be readily modified. It is therefore necessary to remove unwanted cysteine residues and/or insert a cysteine residue into the desired position using molecular biology techniques.

High resolution protein structures or high quality homology models will greatly facilitate the decision making. Care needs to be taken to ensure that the modification does not significantly affect the biophysical properties of the macromolecule.

The selection of an appropriate donor/acceptor pair also needs some consideration although there are many donor/acceptor pairs that have been characterised with some molecules being specifically designed for use in FRET experiments. It is important that there is sufficient overlap between the emission spectrum of **D*** and the absorption spectrum of **A**. A commonly used donor/acceptor pair used for this application is Cy3 and Cy5.

Prior to running a stopped-flow FRET experiment, it is usually necessary to establish the steady state FRET characteristics of reacting components, allowing for a sensible design of the stopped-flow experiment. For example, consider a system in which species 1 (**S1**) is labelled with donor molecule (**D**): (**S1D**) and species 2 (**S2**) is labelled with acceptor molecule (**A**): (**S2A**). A titration can be performed that monitors the change in fluorescence intensity of **D*** (exciting the sample at **D**'s absorption maximum) as a function of concentration of **S2A**. E_{FRET} can be calculated using equation (2).

$$E_{FRET} = 1 - \frac{I_{DA}}{I_D} \qquad (2)$$

Where I_{DA} and I_D represent the fluorescence intensity of the donor with and without the acceptor, respectively. It is also desirable to perform a control experiment to assess whether unlabelled **S1** has an effect on the emission intensity of **S2D***. This ensures that a change in fluorescence intensity of **D*** is not attributed to FRET. A schematic of a typical FRET experiment using an SX series spectrometer is shown in Figure 1.

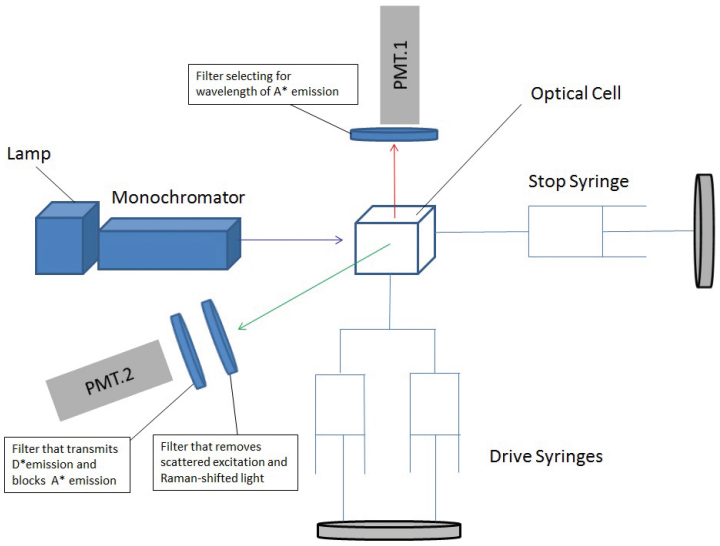

Figure 1. Typical set-up of a stopped-flow FRET experiment. Adapted from Reference[2]

Two photomultiplier detectors (PMT.1 and PMT.2) are set up perpendicular to the excitation beam. It is not essential to have two PMTs however this set up will allow simultaneous measurement of both **D*** and **A***'s emissions. It is imperative that appropriate filters are selected to ensure that the intended emitted light is detected and light from all other sources is minimized. The choice of filters is therefore largely dependent on the donor/acceptor pair being studied. The excitation light will be scattered by the solution and therefore needs to be removed by filters. It is recommended to measure the light throughput at the excitation wavelength of the buffer in absence of fluorophore, with the selected filter in place as this will help determine whether the selected filter is effective in removing scattered light.

LITERATURE REVIEW

The following examples are summaries of published work. For more details, see the associated references.

KINETICS OF PROTEIN-LIGAND INTERACTIONS

Reference[3] - Gakamsky, D.M. et al. Kinetic evidence for a ligand-binding-induced conformational transition in the T cell receptor. *Proceedings of the National Academy of Sciences of the United States of America* 104, 16639-44 (2007).

This example describes how stopped-flow FRET can obtain useful kinetic and mechanistic information regarding complex biomolecular interactions. Stopped-flow FRET has been used to study the interaction between T-cell receptors (TCRs) and their target peptide ligands which are known as pMHCs (major histocompatibility complexes bound to a particular peptide). The study, described in Reference[3], determined the kinetics of the binding interaction between a TCR specific for Cytomegalovirus Peptide (TCR_{CMV}) and its ligand pp65-HLA-A*201. The TCR was labeled with tetramethylrhodamine (acceptor) and the pMHC was labeled with fluorescein (donor).

It was found that the interaction was bi-phasic characterised by a fast step followed by a much slower step. This is demonstrated in the kinetic traces observed on different timescales. Figure 2A shows a representation of the published data of the decrease in donor emission as the binding interaction proceeds over a long timescale. The decrease in emission intensity of the donor can be attributed to a binding interaction as the donor/acceptor pair are brought together, decreasing the distance between them. Figure 2B shows the trace obtained with a much higher temporal resolution. Figure 2C shows an equivalent trace obtained from measuring the increase in fluorescence intensity of the acceptor. The observed traces can be treated as a direct observation of the binding interaction and those in Figure 2A and B can be fit to obtain observed first order rate constants k_2^{obs} and k_1^{obs} for the fast and slow phases of the reaction respectively.

Fitting longer timescale traces needs the addition of an extra rate constant (k_3^{obs}) to account for photobleaching of fluorescein. Equally, the rate constants can be extracted from the acceptor emission traces as seen in Figure 2C. It was determined that k_2^{obs} showed a linear dependence on the concentration of labelled TCR_{CMV} under pseudo first order conditions ([TCR_{CMV}]>>[pMHC]) whereas k_1^{obs} showed no such dependence.

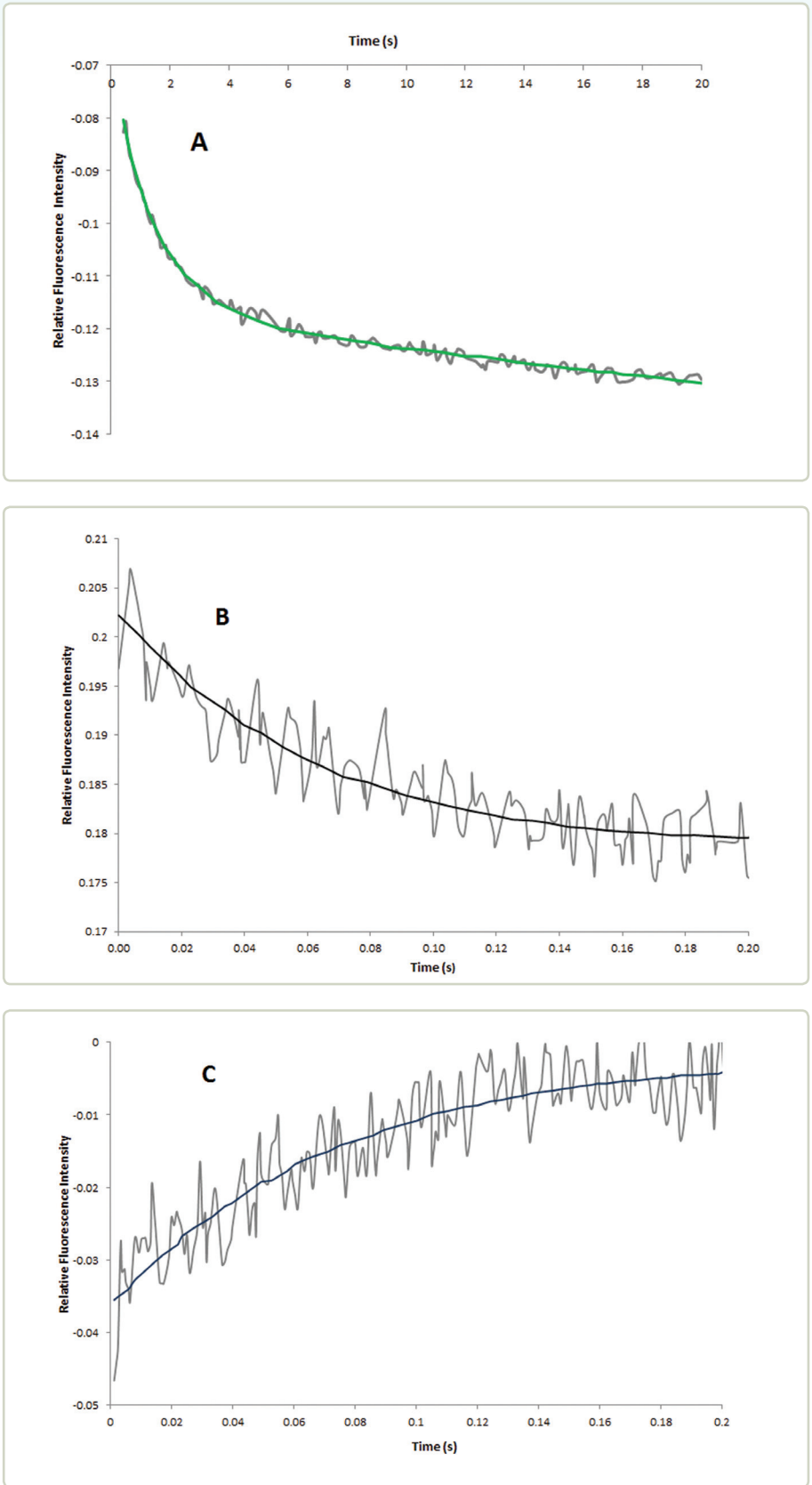

Figure 2. Representation of the data acquired in Reference [3]
A Long timescale monitored at donor emission wavelength
B Short timescale monitored at donor emission wavelength
C Short timescale monitored at donor emission wavelength

Applying these results to those from previous crystallographic studies, the following reaction scheme is implied.

$$\text{TCR} + \text{pMHC} \underset{k_{21}}{\overset{k_{12}}{\rightleftharpoons}} (\text{TCR---pMHC})^{tr} \underset{k_{32}}{\overset{k_{23}}{\rightleftharpoons}} (\text{TCR---pMHC})^{st}$$

Where $(TCR---pMHC)^{tr}$ and $(TCR---pMHC)^{st}$ represent a transient and stable complex respectively. The fact that the first step in the above mechanism is independent of [TCR] (when [TCR]>>[pMHC]) implies that the rapidly formed $(TCR---pMHC)^{tr}$, rapidly dissociates back to the TCR and pMHC. (k_{21} approximately 18-30s^{-1}). The second step of the reaction is much slower (k_{23} approximately 2-4s^{-1}) which represents the transition of the transient complex to a stable TR---pMHC complex and is rate determining. This final step is believed to be brought about by a conformational change in the $(TCR---pMHC)^{tr}$ complex via an "induced fit" mechanism.

MONITORING VESICLE GROWTH

Reference[4]: Budin, I. & Szostak, J.W. Physical effects underlying the transition from primitive to modern cell membranes. *Proceedings of the National Academy of Sciences of the United States of America* 108, 5249-54 (2011).

Stopped-flow FRET was used to demonstrate that fatty acid vesicles which had been doped with phospholipids, competitively acquired fatty acids from equivalent non-phospholipid containing vesicles. The phospholipid containing vesicles therefore grow at the expense of their non-phospholipid containing counterparts. The results of this study may have important implications in understanding the evolution of the cell membrane.

Either fatty acid vesicles or phospholipid containing vesicles were fluorescently labelled with low concentrations of the fluorescent phospholipids "NBD-PE" (Donor) and "Rhodamine-DHPE" (Acceptor) in a 1:1 ratio. The fluorophores are assumed to remain on the surface of the vesicle throughout the experiment. In this study, the authors convert their fluorescence intensity measurements into a relative surface area measurement. This is a valid assumption because a decrease in FRET corresponds to an increase in Donor emission and decrease in Acceptor emission, meaning there has been an increase in the distance between the flourophores i.e. the vesicle has acquired fatty acids resulting in growth and thus, a larger surface area. The origin of the FRET signal is exemplified in Figure 3.

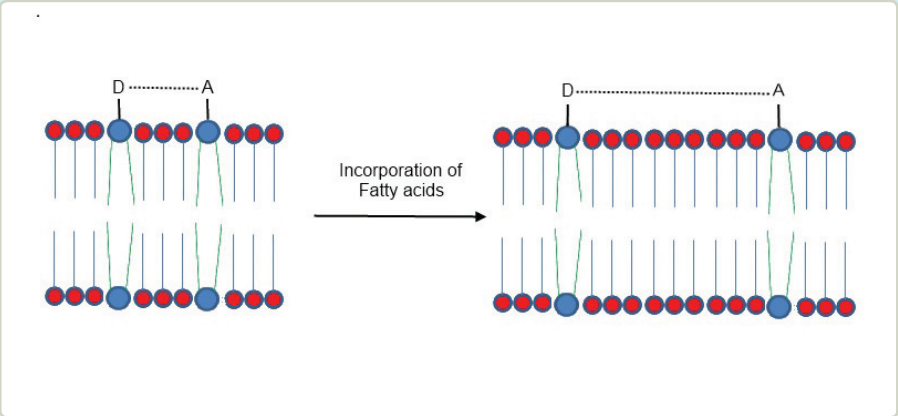

Figure 3. Representation of a segment of a fatty acid vesicle containing a donor (D) and an acceptor (A) fluorescent phospholipids. Fatty acids are represented by red circles with blue tails and fluorescent phospholipids are represented by blue circles with green tails. As the surface area increases, the distance between D and A will also increase.

Relative surface area is calculated from the ratio of the donor fluorescence to the acceptor fluorescence (F_{don}/F_{acc}) from which the relative surface area can be estimated by using a standard curve.[5]

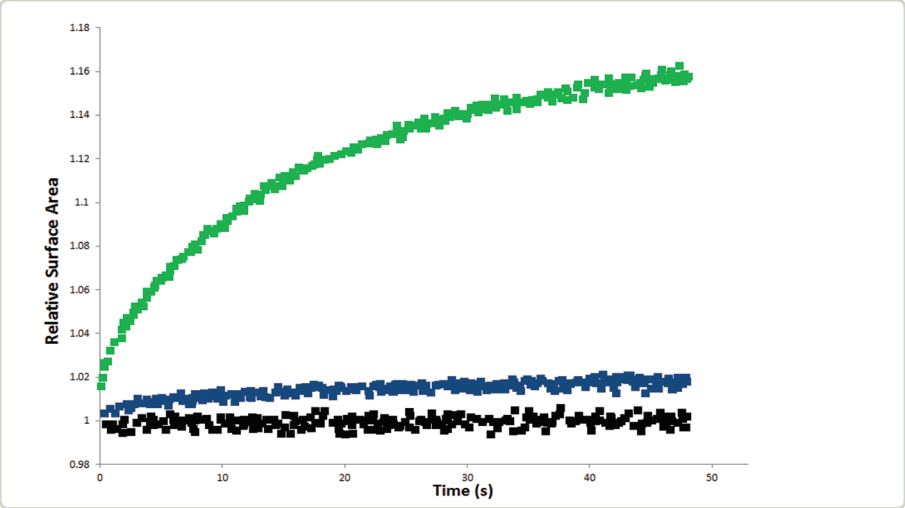

Figure 4. Representation of data presented in Reference[4], showing the change of the phospholipid-fatty acid's relative surface area. Relative surface area was calculated from F_{don}/F_{acc} which can be fit to a standard curve. The labelled phospholipid-fatty acid vesicle (10% phospholipid) was rapidly mixed with: equimolar unlabelled fatty acid vesicles (green curve), buffer (black curve), and an equimolar unlabelled equivalent phospholipid - fatty acid vesicle (blue curve).

Figure 4 shows a representation of the data obtained when the labelled phospholipid-fatty acid vesicle (10% phospholipid) was rapidly mixed with: unlabelled equivalent fatty acid vesicles (green curve), buffer (black curve), and unlabelled equivalent phospholipid - fatty acid vesicles (blue curve).

The green curve shows that when the phospholipid containing vesicle is mixed with the equivalent fatty acid vesicle, the phospholipid containing vesicle grows, i.e. competitively obtains fatty acids form the fatty acid vesicle. Figure 5 shows a representation of the data obtained when the labelled fatty acid vesicle is mixed with the unlabelled phospholipid containing vesicle (blue curve), an equimolar amount of equivalent unlabelled fatty acid vesicle (green line), and buffer (black line).

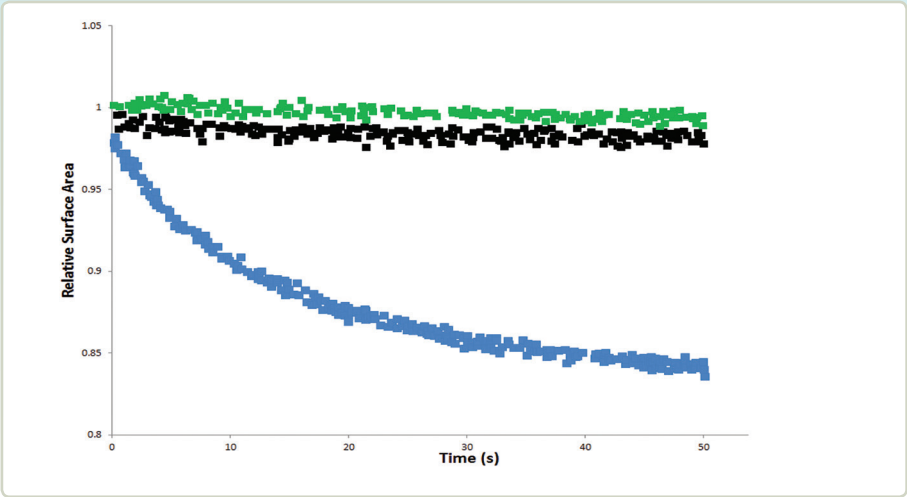

Figure 5. Representation of data presented in Reference[4], showing the change of the fatty acid's relative surface area. Relative surface area was calculated from F_{don}/F_{acc} which can be fit to a standard curve. The labelled fatty acid vesicle is mixed with the unlabelled phospholipid containing vesicle (blue curve), an equimolar amount of equivalent unlabelled fatty acid vesicle (green line), and buffer (black line).

The data in Figure 5 further support the competitive growth of the phospholipid containing fatty acid vesicles. If the earliest cell membranes were composed of fatty acid vesicles (as currently suspected), the presence of small proportions of phospholipids may have provided a selective advantage for these cells to grow. This may have driven the conversion from primitive to modern cell membranes.[4]

KINETICS OF NUCLEOSOME STRUCTURAL DYNAMICS

Reference[5]: Li, G., Levitus, M., Bustamante, C. and Widom, J. Rapid spontaneous accessibility of nucleosomal DNA. *Nature Structural and Molecular Biology* 12, 46-53 (2005).

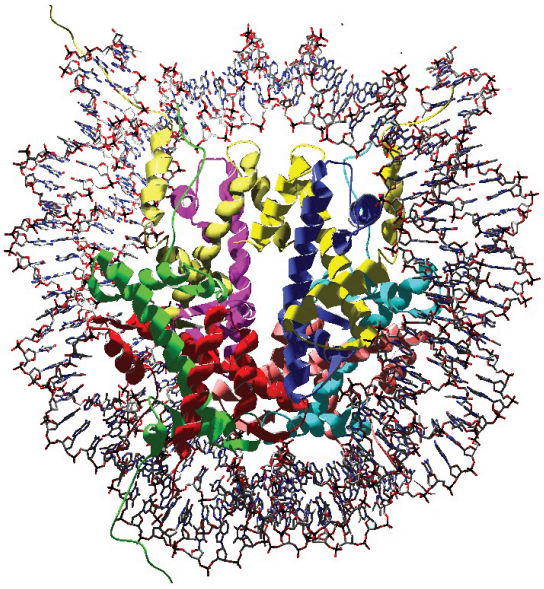

Figure 6. X-ray crystal structure of a nucleosome. Each subunit of the histone octomer is coloured differently. PDB ID - 1AOI

In the nucleus of eukaryotic cells, the genomic DNA is organised into a structure called chromatin that consists of repeating units called nucleosomes. An individual nucleosome consists of an octomeric protein called a histone which the DNA wraps around. (Figure 6) For many essential biological processes including transcription and transcription regulation, the DNA surface needs to be accessible so that other species can interact with it.

Therefore, the nucleosome must unwrap so that these events can occur. The rate at which unwrapping/rewrapping occurs therefore has a direct effect on processes that govern an organism's metabolism. Stopped-flow FRET was used to determine the kinetics of DNA unwrapping from the nucleosome, giving important insights into the biological processes mentioned above.

A 147 base pair DNA sequence containing a binding site for the transcription factor LexA was used to prepare nucleosomes. In addition, this DNA strand had a Cys3 (donor) group attached to its 5' end. The histone protein was labelled with Cys5 (acceptor) so that changes in distance between the DNA and the Histone could be observed with a change in FRET signal. In the wrapped nucleosome the DNA binding site is buried within the structure. However, when the nucleosome becomes transiently unwrapped, the DNA binding site is exposed. In the presence of LexA, the unwrapped nucleosome becomes 'trapped' in its unwrapped state due to the fact that transcription factors generally bind target DNA sequences extremely rapidly and tightly. The unwrapped nucleosome exhibits a decreased FRET efficiency, allowing this process to be observed using stopped-flow spectroscopy by rapidly mixing the nucleosome with LexA. When there is a large excess of LexA, it can be assumed that the observed first order rate constant corresponds to the rate of unwrapping. A representation of the kinetic data published is shown in Figure 7.

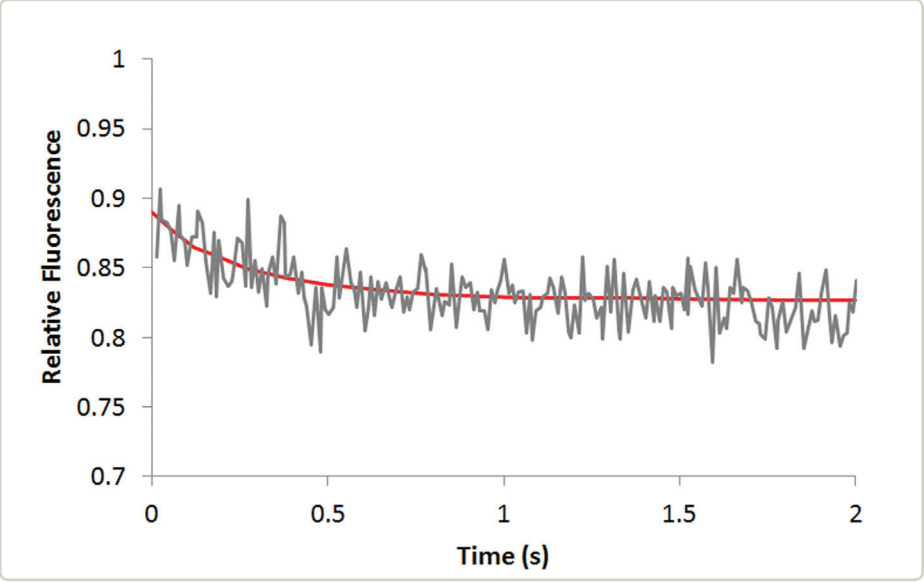

Figure 7. Representation of data published in Reference[6].

A value of approximately $4s^{-1}$ was obtained for the first order rate constant. The equilibrium constant between wrapped and unwrapped states has been previously been determined using steady state FRET experiments (K_{eq} ~4.5×10^{-2}). This allows an estimation of the reverse re-wrapping process via the relationship:

$$K_{eq}=k_1 / k_{-1}$$

This gives a rewrapping rate constant of ~$90s^{-1}$. These rate constants correspond to lifetimes of approximately 250ms and 10ms for the wrapped and un-wrapped forms of the nucleosome respectively. There is good reason to believe that the data acquired in this study are representative of nucleosomes contained in an extended chromatin structure.

REFERENCES

1. Selvin, P.R. The renaissance of fluorescence resonance energy transfer. *Nature Structural Biology* 7, 730-4 (2000).

2. Tims, H.S. & Widom, J. Stopped-flow fluorescence resonance energy transfer for analysis of nucleosome dynamics. *Methods* (San Diego, Calif.) 41, 296-303 (2007).

3. Gakamsky, D.M. et al. Kinetic evidence for a ligand-binding-induced conformational transition in the T cell receptor. *Proceedings of the National Academy of Sciences of the United States of America* 104, 16639-44 (2007).

4. Budin, I. & Szostak, J.W. Physical effects underlying the transition from primitive to modern cell membranes. *Proceedings of the National Academy of Sciences of the United States of America* 108, 5249-54 (2011).

5. Hanczyc, M.M., Fujikawa, S.M. & Szostak, J.W. Experimental models of primitive cellular compartments: encapsulation, growth, and division. *Science* (New York, N.Y.) 302, 618-22 (2003).

6. Li, G., Levitus, M., Bustamante, C. & Widom, J. Rapid spontaneous accessibility of nucleosomal DNA. *Nature Structural and Molecular Biology* 12, 46-53 (2005).

AppliedPhotophysics

Ultrasensitive Spectroscopy for the Life Sciences

4140Q009 v. 2

Applied Photophysics Ltd,
21, Mole Business Park, Leatherhead, Surrey, KT22 7BA, UK
Tel (UK): +44 1372 386 537
Tel (USA): 1-800 543 4130
Fax: +44 1372 386 477

Applied Photophysics was established in 1971 by
The Royal Institution of Great Britain

www.photophysics.com